An Archaean sill complex and associated supracrustal rocks, Arveprinsen Ejland, north-east Disko Bugt, West Greenland

Brian Marshall and Hans Kristian Schønwandt

Archaean supracrustal rocks on Arveprinsen Ejland comprise mafic and felsic volcanic rocks overlain by an epiclastic sedimentary sequence invaded by a mafic to ultramafic sill complex. The latter has a strike-length of 7500 m and a cumulative preserved thickness of 2000–2500 m and amounts to nearly 50% of the exposed thickness of the supracrustal rocks. Chilled and locally peperitic contacts are developed between component sills and the inter-sill metasedimentary septa. The sub-alkalic sill complex and mafic lavas and tuffs are high-magnesium tholeiites and basaltic komatiites whereas the felsic rocks are calc-alkaline rhyolites and dacites. Chondrite- and MORB-normalised spider diagrams affirm the close similarity of the mafic volcanic rocks and the sill complex; they are also consistent with a tholeiitic or komatiitic affinity. Tectonomagmatic discrimination plots suggest an ensialic arc-related setting for the sill complex and the mafic and felsic volcanic rocks.

The sill complex was progressively emplaced, as an upward-younging sequence of component sills, beneath 2 to 2.5 km of seawater and substantially less than 0.5 km of wet sediment. Sills formed when the magmatic pressure exceeded the *effective* overburden pressure of the sediment plus the vertical tensile strength (T_o) of the host materials. Intrusion was probably promoted by the drop in T_o at the interface between contact-lithified and poorly lithified strata. The thickness of the sill complex was accommodated by dilational lifting plus the capacity of an intrusion to create space through expulsion of water from wet sediment.

B.M., *Department of Applied Geology, University of Technology, Sydney, P. O. Box 123 Broadway, N.S.W. 2007, Australia*. E-mail: *Brian.Marshall@uts.edu.au*.
H.K.S., *Geological Survey of Denmark and Greenland, Thoravej 8, DK-2400 Copenhagen NV, Denmark*. Present address: *Government of Greenland, Bureau of Minerals and Petroleum, DK-3900 Nuuk, Greenland*.

Keywords: Archaean, Disko Bugt, geochemistry, sill complex, subvolcanic rocks, supracrustal rocks, West Greenland

The rocks of Arveprinsen Ejland, Disko Bugt, central West Greenland (Fig. 1) were divided by Escher & Burri (1967) into an infrastructure of 'Jacobshavn gneiss' and 'Atâ granite' (Atâ Tonalite on the geological map of Garde 1994), and a suprastructure termed the 'Anap nunâ Group'. Kalsbeek *et al.* (1988) demonstrated that, at least for north-eastern Arveprinsen Ejland, the supracrustal rocks are Archaean and distinct from the Proterozoic supracrustal sequence that occurs east of Arveprinsen Ejland.

The Archaean supracrustal rocks of north-eastern Arveprinsen Ejland (henceforth called the Arveprinsen supracrustals) comprise a metamorphosed sequence of massive to pillowed basaltic flows and mafic tuffs, with subordinate felsic volcanic rocks, overlain by and gradational into an epiclastic sedimentary sequence, also with felsic volcanic rocks. Metamorphosed and deformed mafic sills (herein termed a sill complex) totally dominate the upper portion of the supracrustals. Two distinctly younger sets of mafic dykes cut the entire sequence. The older set is inter-kinematic and the younger is post-kinematic with respect to the

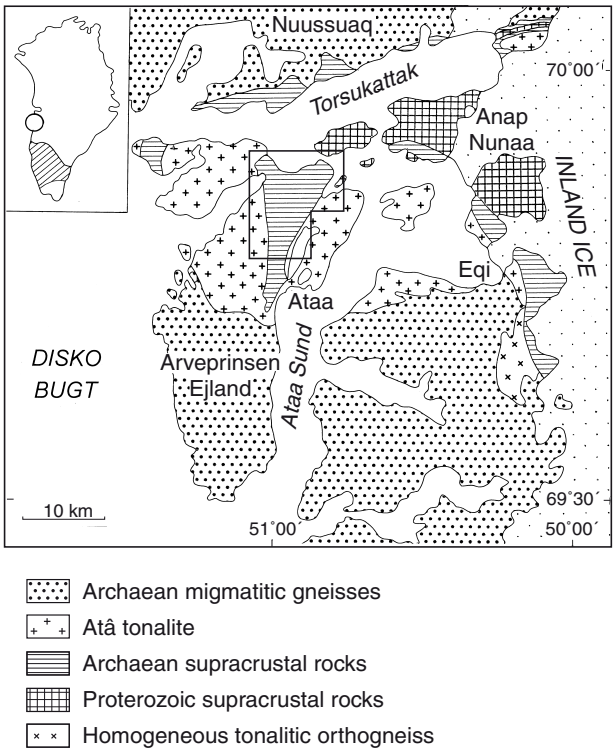

Fig. 1. Simplified geological map of the Ataa Sund region (after Kalsbeek 1990) with the investigated area outlined. The inset shows the location (circled) in central West Greenland, north of the Archaean craton (oblique ruling).

polyphase deformation history, which comprises at least four folding events (Marshall & Schønwandt 1990).

The supracrustal rocks have undergone at least one phase (but probably two phases) of regional metamorphism. The resulting greenschist and amphibolite facies assemblages define a south-closing form within the Atâ granite (Knudsen *et al.* 1988). The metamorphic facies boundary is approximately parallel to primary layering on the west of the structure, but it is discordant on the east side where the contact truncates the layering.

Sill complexes are known from other Archaean metavolcanic-metasedimentary greenstone belts (e.g. Naldrett & Mason 1968; Jaques 1976; Raudsepp & Ayres 1982). They are typically emplaced at a high crustal level, provide samples of magmas which probably were the source of the spatially associated basaltic lavas, and may be termed subvolcanic (Raudsepp & Ayres 1982). Similar associations of mafic plutonic rocks and mafic volcanites exist in the Proterozoic rocks of southern Finland (Härme 1980; Suominen 1988).

The aims of this paper are to present field observations, petrography and chemical data relating to parts of the sill complex on Arveprinsen Ejland, in order to discuss its emplacement mechanism, and its petrogenetic and tectonic significance.

Field observations

The Arveprinsen supracrustals, including the sill complex, occupy a north- to north-east-trending D_1 regional fold, which is flexed about a WNW-trending D_2 structure (Fig. 2). Because the D_1 fold youngs into its core (Fig. 2) and has a moderate to very steep southward plunge, it is a non-cylindrical antiformal syncline (the Arveprinsen antiform). A more substantial account of the regional and detailed structure is given by Marshall & Schønwandt (1990).

Stratigraphy

The metavolcanic-metasedimentary preserved succession (excluding the sill complex) consists of a lower unit comprising 2500–3000 m of mafic flows and tuffs, and an upper unit variously comprising 500–750 m of feldspathic, siliciclastic and pelitic epiclastic metasedimentary rocks, with developments of disseminated and massive base metal sulphide (Fig. 2). The lower contact is against the intrusive Atâ tonalite and the upper limit is the coastline of Arveprinsen Ejland, so the section is incomplete. In feldspathic (volcaniclastic?) units, the younging directions are based on scour-and-fill structures, cross lamination and rare grading. Where the metasedimentary rocks consist of quartz-rich sandstone and siltstone with variable amounts of pelitic material, younging may be obtained from bottom structures, grading and cross lamination that collectively comprise incomplete Bouma units. The sill complex, as delineated (Fig. 2), is essentially restricted to the metasedimentary part of the succession. It effectively swells the total thickness of the supracrustal section to between 5000 and 6000 m, and constitutes nearly 50% of the stratigraphic column (Fig. 2). In addition to the sill complex, a few thin (< 50 m) sills occur within the metavolcanic portion of the succession.

The boundary between the sill complex and the supracrustals (Fig. 2) has a superficially discordant appearance which masks the dilational nature of the sills. This could be due to: (1) an inability to show, at this scale, the true extent of the interfingering of metasedimentary septa (terminology after Raudsepp & Ayres

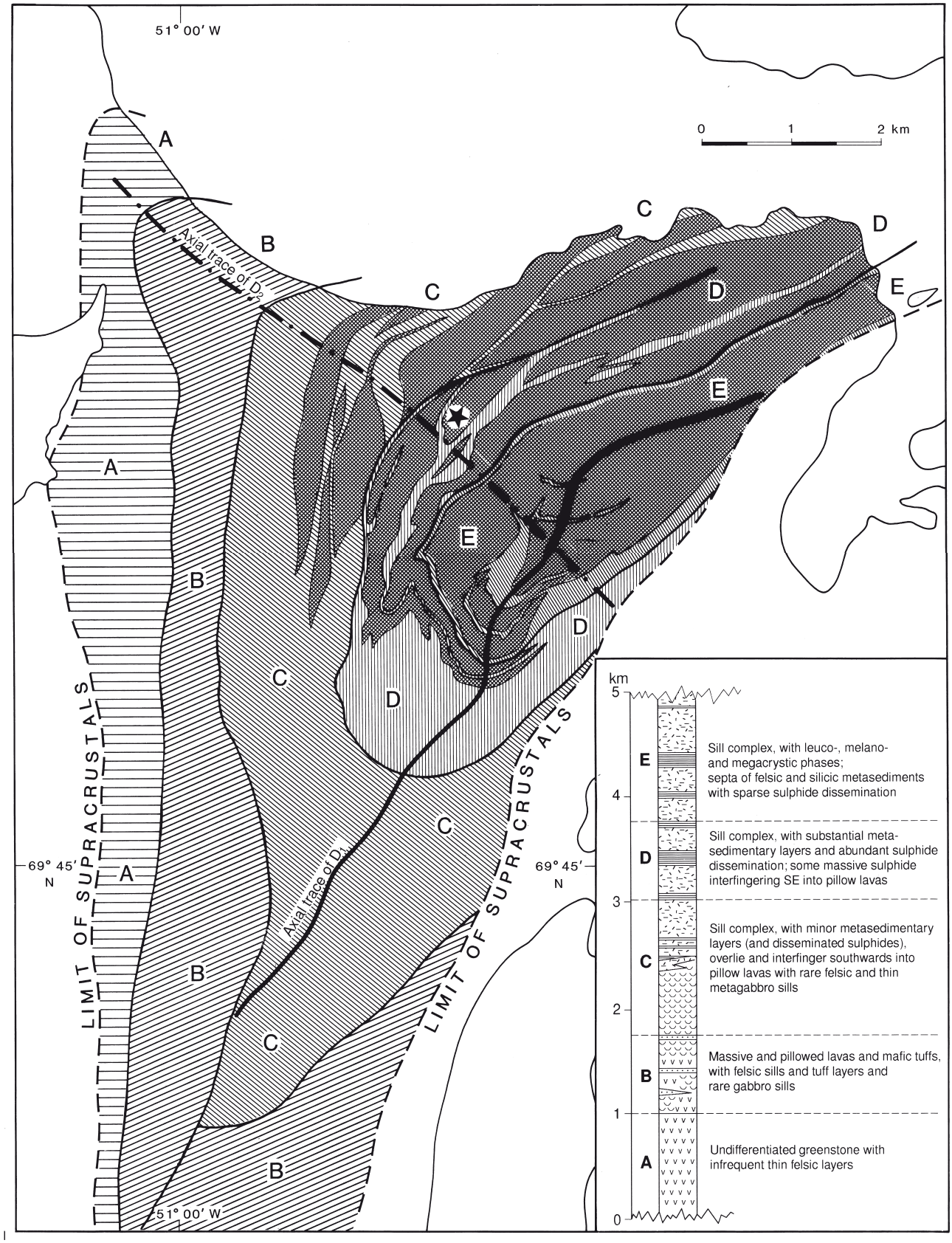

Fig. 2. Interpretative geological map of the sill complex and associated supracrustal rocks, north-eastern Arveprinsen Ejland, with the axial traces of D_1 and D_2 folds (full line and dash-dot line, respectively). The star locates 'Anderson's Prospect'.

1982) and component sills of the sill complex; (2) difficulty experienced in the field in distinguishing between medium- to fine-grained sill rocks and metavolcanics, particularly where the rocks are highly strained and constitute tracts of retrograde greenschist (Knudsen *et al.* 1988); and (3) apparent thickness effects on the western limb of the regional fold caused by dip variation and parasitic folding. The boundary could also result from the sill occupying space created by change of porosity and dissolution accompanying the expulsion of pore-water during contact metamorphism (e.g. Einsele 1980). This and other aspects of sill emplacement are examined in a later section.

Based on reconnaissance mapping, an attempt has been made to indicate component bodies of the sill complex where they are outlined by mappable septa (Fig. 2). The mapping suggests that there are at least eight sills, each differing from the immediately overlying and underlying sills in terms of gross appearance and degree of internal variation. Thus, some of the sills seem to have undergone a degree of post-emplacement differentiation, whereas others show little evidence of significant amounts of crystal-liquid separation following intrusion. In some cases a sill contains cumulate layers of abundant feldspar megacrysts (up to 5 cm across), elsewhere phenocrysts are relatively small (1–3 cm), sparsely distributed, and consistent with *in situ* growth in equilibrium with the melt. Feldspars decrease in size against the inter-sill septa. Lithological and petrographical summaries of the main rock types comprising the sill complex are presented in Table 1.

Contact relationships

The sills have maximum thicknesses (corrected for dip but not strain) ranging very approximately from 200 to 600 m. Their contacts and internal layering are parallel to the bedding in the metasedimentary sequences, consistent with their emplacement as pre-orogenic sills within a flat-lying stratigraphy. Chilled margins were recorded at upper, lower and lateral contacts. They most probably surround each sill, but this could not be proved because the majority of contacts are shear zones marked by retrograde schist development.

Component sills may be in direct contact with each other at their upper and lower contacts, but they are more typically separated by metasedimentary inter-sill septa which, although they range up to 150 m in thickness, are usually < 50 m thick. Towards the interpreted lateral contacts, thinner (< 20 m), discontinuous, more closely spaced septa are encountered. These are either intra-sill, and result from interfingering of magma at the margin, or they separate closely related (in time and composition) magma pulses which combined to build a substantial sill unit. In some cases, thin septa obliquely separate two sills between shared inter-sill septa.

Uncommon features of the contacts include small (< 1 m) cuspate and lobate magmatic incursions, and larger (up to 10 m) irregular and planar discordances where bedding in the septum is obliquely truncated. In one such instance of oblique truncation, younging reversed along the contact but D_1 vergence remained constant. This suggests that soft-sediment folding preceded or was penecontemporaneous with sill emplacement.

From the contacts examined in detail, there is no quantifiable correlation between the type of contact (whether upper, lower or lateral) and the thickness of the chilled border zones, although the better preserved marginal assemblages do seem to be on the lower contacts. In general, 20–50 cm of extremely fine-grained 'flinty-looking' intrusive rock pass into 1 to 5 m of medium-grained rock which, with increasing grain size, passes imperceptably into the main body of the sill. Where the latter is porphyritic, both matrix and phenocryst grain size progressively coarsen; where non-porphyritic, the rock becomes spotty or blotchy due to retrogression of coarse mafic phases, and in some cases is coarsely poikiloblastic.

Sedimentary rocks at the contact have a chert-like aspect and, depending on the degree of hornfelsing and silica metasomatism, may or may not be overprinted by the D_1 foliation and lineation. Particularly at lower contacts, up to 0.5 m of recrystallised and silicified sedimentary rock are fractured and healed by vein quartz. Although generally sharp and planar, the contact may be locally (over a few metres) irregular and ill-defined due to incorporation of soft sediment in the base of the sill, and sill clasts within the sediment. This mutual invasion has resulted in irregularly developed globular, fluidal peperitic zones (Brooks *et al.* 1982; Busby-Spera & White 1987), even though peperites are more typical of higher viscosity andesitic magma (Kokelaar 1982). Other than on the scale of the thin peperitic zones, the sill complex lacks metasedimentary xenoliths or rafts (cf. Knudsen *et al.* 1988).

Table 1. Lithology and petrography of representative rock types from the sill complex

Rock type	Lithology and petrography
Porphyritic metabasite (1, 2)*	Equant and prismatic feldspar phenocrysts (up to 2 cm across) are sparsely distributed (spacing in the order of 1 per 100 cm^2) in a fine- to medium-grained (2 to 4 mm) green-grey metabasite – typically unfoliated and unlineated. The metabasite exhibits remnant poikilitic to ophitic igneous textures. Poikiloblasts of amphibole (up to 6 mm, weakly pleochroic from very pale green to colourless, oblique extinction) enclose laths (up to 0.5 mm) of saussuritized feldspar. The matrix comprises metamorphic feldspar, epidote-group minerals, chlorite, sphene, amphibole needles and minor carbonate.
Megacrystic metabasite	Equant euhedral to near spherical calcic plagioclase megacrysts (up to 5 cm across) are abundantly distributed (3 to 4 per 100 cm^2) in layers up to 2 m thick within a metabasite matrix. The matrix is as above.
Metagabbro and metadolerite (3, 6, 7)*	Speckled rocks comprising dark grey prismatic mafic grains (up to 7.5 mm) in a felsic matrix – approximate proportions 50:50 – weakly foliated to unfoliated, but in some cases well lineated. The texture is metamorphic. The prismatic to ragged amphibole crystals (strongly pleochroic from blue-geen to yellow-green) exhibit linear preferred orientation in a finer grained (up to 2 mm) matrix of plagioclase, chlorite, granular epidote, amphibole, minor sphene and uncommon calcite.
(Meta-)leuco-gabbro and leucodolerite	Speckled rocks similar to metagabbro and metadolerite; but mafic to felsic proportions approximate 40:60, the mafic component is pale to medium grey, and foliation and lineation range from strong to absent. Remnant ophitic igneous texture eucodolerite exists where foliation/lineation are lacking. The pale anhedral amphibole is weakly pleochroic from very pale green to colourless.
(Meta-)melano-gabbro and melanodolerite	Melanocratic rocks comprising a dark grey mafic component and an interstitial felsic matrix in approximate 60:40 proportions. The texture is totally metamorphic. The amphibole (intense pleochroism from blue-green to yellow-green, oblique extinction, up to 6 mm) forms decussate ragged prisms and sheaves associated with plagioclase and minor biotite. Chlorite, epidote, sphene and calcite are absent.
Poikiloblastic metagabbro (9, 10, 11)*	Pale to medium grey medium-grained (up to 5 mm) speckly rock with poikiloblastic patches up to 4 cm across – generally unfoliated and unlineated. The igneous poikilitic texture is pseudomorphed by poikiloblastic amphibole after pyroxene.The amphibole (weakly pleochroic, oblique extinction) encloses plagioclase laths. These and the feldspathic matrix are altered to a saussuritic aggegate of epidote goup minerals, chlorite, sphene, amphibole needles and minor calcite.
Spotted metagabbro (4, 5, 8)*	Pale to medium grey rock with closely spaced (4 to 6 per 9 cm^2) dark grey elliptical blotches (0.5 to 1 cm across) which commonly define the foliation and lineation The blotches are masses of oriented fine-grained (0.5 mm to 1 mm) chlorite and minor zoisite (?). They are separated by a matrix of metamorphic plagioclase, abundant carbonate, epidote group minerals, sphene and amphibole needles.

* Analysis numbers from Table 2.

Table 2. Chemical composition of representative samples from the sill complex and associated mafic and felsic volcanic rocks

	Mafic sill complex													
Analysis	1	2	3	4	5	6	7	8	9	10	11	12	13	14
GGU No	362646	362681	362679	362678	362677	362697	362698	362699	362700	362659	362661	362687	362689	362682
SiO_2	46.28	47.83	47.70	46.07	43.02	50.29	44.32	46.50	44.00	47.43	48.57	49.75	48.58	50.16
TiO_2	1.05	0.96	1.02	0.86	0.76	0.62	0.55	0.37	0.56	0.59	0.76	0.61	0.43	0.58
Al_2O_3	15.34	14.81	15.81	16.12	14.89	16.08	13.57	14.83	14.00	15.48	18.35	14.79	17.02	13.52
Fe_2O_3	1.98	0.33	1.11	0.79	0.89	0.75	0.75	0.86	0.99	1.78	2.15	2.45	2.19	1.31
FeO	9.66	10.53	9.82	9.73	9.52	7.32	9.71	7.40	8.57	7.13	5.57	6.25	4.27	7.12
MnO	0.17	0.16	0.18	0.17	0.17	0.11	0.16	0.13	0.14	0.16	0.14	0.14	0.11	0.16
MgO	7.46	7.24	7.95	8.13	8.16	10.02	16.01	13.87	13.84	8.51	6.35	8.39	7.91	8.76
CaO	8.97	8.84	9.62	10.77	9.40	5.91	7.50	8.97	8.26	12.83	11.76	12.08	13.57	12.96
Na_2O	2.31	3.47	2.13	1.85	1.64	3.75	1.25	1.40	1.06	1.56	2.93	2.46	2.03	2.14
K_2O	0.34	0.33	0.15	0.05	0.11	0.04	0.15	0.14	0.03	0.03	0.09	0.04	0.02	0.04
P_2O_5	0.07	0.07	0.04	0.06	0.04	0.04	0.04	0.03	0.04	0.03	0.09	0.04	0.02	0.03
volatiles	5.43	4.85	4.24	5.13	11.09	4.28	5.67	5.22	7.76	4.11	2.90	2.83	3.34	3.12
Tot.(%)	99.07	99.41	99.78	99.74	99.69	99.22	99.68	99.72	99.25	99.64	99.66	99.82	99.49	99.91
mg´	0.54	0.54	0.57	0.58	0.59	0.69	0.73	0.75	0.72	0.64	0.60	0.65	0.69	0.64
Rb	11	8	4.2	1.3	2.3	<0.5	2.3	3.2	0.5	<0.5	1.6	<0.5	<0.5	0.7
Ba	76	83	59	16	29	18	33	60	6	7	20	12	12	19
Pb	18	10	12	11	10	10	8	6	7	7	7	7	6	8
Sr	107	101	113	98	56	119	72	81	82	88	91	107	101	131
La	3	7	4	3	<1	8	4	3	3	<1	3	3	2	<1
Ce	10	12	7	10	6	17	6	6	7	7	11	8	11	6
Nd	7	8	5	6	4	8	3	2	4	4	8	6	5	4
Y	23	21	20	18	14	15	11	8	11	13	21	13	12	13
Th	<1	<1	<1	<1	<1	2	<1	<1	<1	<1	<1	<1	<1	<1
Zr	55	53	54	46	32	65	34	24	31	23	46	30	28	30
Nb	2.5	2.8	2.8	2.5	2.1	3.1	1.8	1.5	1.6	1.9	2.4	2	1.8	1.9
Zn	373	442	404	141	161	112	152	99	99	104	72	73	71	125
Cu	140	13	13	115	41	105	39	34	90	21	7	56	51	45
Co	53	46	49	59	60	53	85	72	76	56	41	53	52	47
Ni	126	129	145	191	214	233	638	457	559	192	70	87	80	89
Sc	38	39	38	33	26	29	25	13	20	37	43	53	55	54
V	306	281	282	260	223	203	192	112	177	232	229	258	269	252
Cr	312	267	323	286	322	608	1690	381	1090	435	544	423	429	544
Ga	19	18	17	18	15	16	14	10	13	15	18	15	14	14

Major elements analysed by XRF on glass discs at the Survey (Na by AAS); trace elements analysed at the Geological Institute, University of Copenhagen, by XRF on powder tablets.

Table 2 *(continued)*

Associated mafic volcanic rocks							Associated felsic volcanic rocks									
15	16	17	18	19	20	21	22	23	24	25	26	27	28	29	30	Analysis
362694	362695	362663	362652	362684	362685	362686	362601	362602	362657	362656	362664	362709	362732	362743	362745	GGUNo
49.15	47.86	46.32	48.74	47.83	52.51	50.35	68.00	69.80	65.63	73.42	68.97	70.80	71.11	70.04	65.73	SiO_2
1.43	1.46	1.03	0.68	0.59	0.55	0.60	0.30	0.26	0.41	0.28	0.27	0.27	0.24	0.24	0.45	TiO_2
14.62	14.84	12.18	17.10	14.88	14.29	14.96	15.17	14.76	15.04	13.75	15.30	14.20	15.35	15.01	16.57	Al_2O_3
2.06	2.34	0.73	1.36	0.97	0.98	0.39	0.00	0.37	2.10	0.52	0.32	0.28	0.14	0.08	0.37	Fe_2O_3
10.12	10.18	10.84	8.69	9.23	8.12	8.25	2.09	1.48	3.67	1.70	1.26	1.59	1.56	1.39	2.93	FeO
0.20	0.25	0.21	0.16	0.17	0.16	0.17	0.04	0.02	0.03	0.01	0.03	0.04	0.03	0.03	0.04	MnO
7.30	6.41	5.97	9.12	11.55	10.16	7.67	1.16	0.93	2.30	1.35	0.87	1.29	0.79	0.90	1.55	MgO
8.94	10.35	8.96	5.10	6.54	6.22	6.41	3.30	2.09	1.92	1.32	2.40	2.08	2.09	2.29	4.09	CaO
2.14	1.88	1.66	2.08	1.97	1.87	3.66	5.04	6.18	5.21	4.58	4.59	4.73	5.77	5.22	5.05	Na_2O
0.09	0.15	0.04	1.27	0.06	0.04	0.08	1.50	0.98	0.59	1.26	2.15	1.71	1.21	1.86	1.14	K_2O
0.14	0.14	0.07	0.03	0.03	0.03	0.04	0.09	0.08	0.15	0.14	0.07	0.09	0.06	0.06	0.08	P_2O_5
3.79	3.59	11.14	5.55	5.99	4.72	6.71	2.69	2.21	2.38	1.55	2.80	1.93	1.04	1.73	1.46	volatiles
99.98	99.46	99.15	99.88	99.81	99.65	99.29	99.38	99.15	99.43	99.88	99.03	99.01	99.4	98.85	99.46	Tot(%)
0.52	0.48	0.48	0.62	0.67	0.67	0.61	0.50	0.48	0.42	0.53	0.50	0.56	0.46	0.52	0.46	mg´
1.7	2.5	1	44	1.2	0.6	1.5	43	21	14	25	49	42	34	46	38	Rb
17	35	13	297	27	14	39	334	355	130	164	492	687	548	469	270	Ba
10	16	11	18	15	14	71	7	6	7	8	6	6	11	10	7	P
95	117	106	99	117	127	86	231	112	93	104	177	95	385	335	262	Sr
6	5	3	4	5	4	44	14	23	35	23	25	22	14	11	12	La
15	16	13	10	9	13	81	32	39	65	47	42	44	27	22	22	Ce
11	9	6	6	4	6	32	15	18	29	19	17	20	12	10	12	Nd
32	33	24	18	13	12	11	6	4	15	9	4	6	4	4	9	Y
2	2	<1	nd	1	<1	<1	4	6	6	9	7	6	4	4	4	Th
100	100	59	49	45	50	39	89	109	128	116	116	89	96	82	103	Zr
5.2	5.1	3.3	2.6	2.6	2.5	2.2	3.1	2.5	5.1	4.2	2.4	4	1.8	2.2	4	Nb
152	216	194	282	425	296	633	41	32	100	37	32	42	33	38	35	Zn
17	79	75	39	62	52	14	6	7	387	123	6	<2	9	<2	24	Cu
61	59	52	53	54	51	106	55	37	72	37	14	16	35	34	33	Co
124	127	57	213	303	281	309	11	10	38	21	9	15	8	9	19	Ni
40	41	58	30	30	26	28	6	4	11	4	4	6	2	4	10	Sc
322	332	379	218	211	181	185	47	33	77	31	37	42	32	31	76	V
275	273	264	538	817	705	872	27	53	85	19	21	37	15	17	43	Cr
19	19	16	17	16	15	10	17	17	20	16	18	18	17	16	18	Ga

Petrography and chemistry

Significant proportions of the petrography and chemistry pertain to the sill complex. Petrographic notes and chemical data for the massive and pillowed basalts, and for the mafic tuffs and felsic rocks, enable comparison with the sill complex and with data from other areas. However, the mafic tuffs are both heterogeneous, on a scale of 0.5 m, and intensely altered; their results should therefore be treated cautiously.

Petrography

Primary textures were, in some cases, pseudomorphically preserved in sill complex rocks, but they have usually been overprinted by greenschist- to amphibolite-facies metamorphism and penetrative deformations. The texture therefore now comprises variably orientated assemblages of amphibole, chlorite, feldspar, sphene and carbonate. In terms of the field appearance, seven principal rock types (Table 1) make up the sill complex. All of these rock types, which probably represent igneous precursors with primary layering due to differentiation processes, are not present in each component sill. This could be due to compositional differences in the magma pulses which formed the various component sills, although other factors such as thickness and rate of cooling could also be involved. Systematic evaluation of this and other aspects of the layering are precluded by the intensity of metamorphism and deformation.

Petrochemistry

The major- and trace-element data determined for rocks from the sill complex, and from basalts, mafic tuffs and felsic volcanic rocks intruded by the complex, are presented in Table 2.

Of the 14 rocks analysed from the sill complex, samples 362646, 362677, 362678, 362679 and 362681 (Analyses 1–5, Table 2) are from the same component sill immediately overlying 'Anderson's Prospect' (Marshall & Schønwandt 1990). Sample 362681 (mg′ 0.54) is from the basal chilled contact, 362646 and 362679 (mg′ 0.54 and 0.57 respectively) are within 20 m of the contact but beyond the zone of obvious chilling, and 362677 and 362678 (mg′ 0.59 and 0.58 respectively) are from coarser-grained spotted metagabbro (Table 1) more distant from the contact.

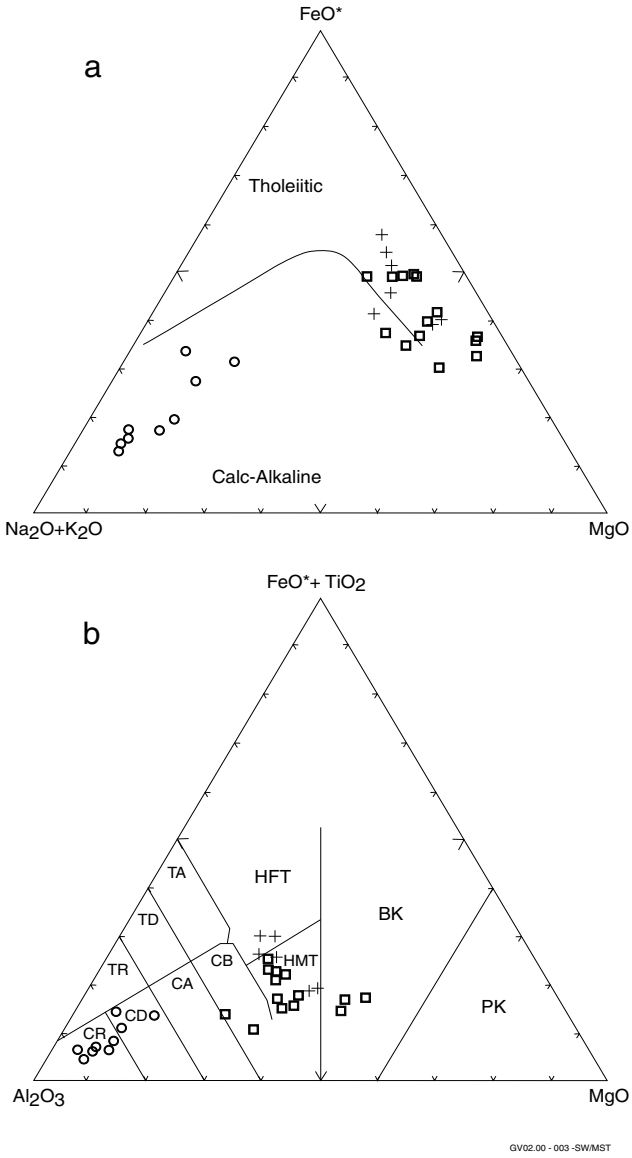

Fig. 3. **a**: AFM diagram for rocks from the sill complex (open squares), mafic volcanics (crosses) and felsic volcanics (open circles). Tholeiite-calc-alkaline division after Irvine & Baragar (1971). **b**: Jensen diagram (Jensen 1976) for rocks from the sill complex, mafic volcanics and felsic volcanics; symbols as for **a**. PK: picritic komatiite; BK: basaltic komatiite; HMT: high magnesium tholeiite; HFT: high-iron tholeiite; CR, CD, CA, CB: calc-alkaline rhyolite, dacite, andesite, basalt; TR, TD, TA: tholeiitic series.

Sample 362659 (Analysis 10, Table 2; mg′ 0.64) is from the next component sill up-sequence from that overlying 'Anderson's Prospect'; poikilitic pyroxene (now pseudomorphed by amphibole) suggests an original cumulate texture.

Samples 362697 to 362700 (Analyses 6–9, Table 2) and samples 362682, 362687 and 362689 (Analyses 12

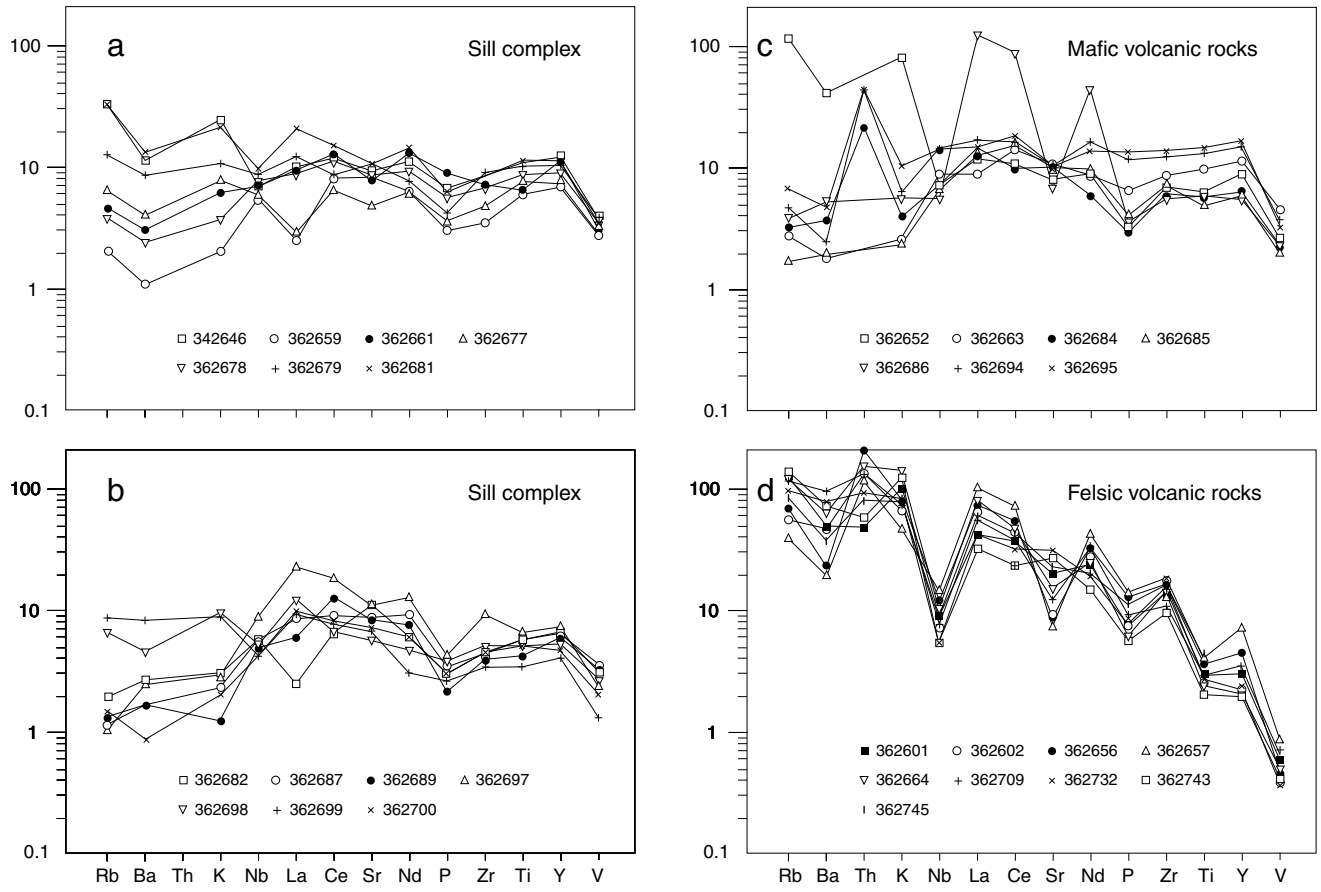

Fig. 4. Chondrite-normalised multi-element spider diagrams for: **a** and **b**: Sill complex samples. **c**: Mafic volcanic samples. **d**: Felsic volcanic samples. Normalised after Thompson *et al.* (1984).

–14, Table 2) are respectively from the basal and upper parts of a component sill underlying and to the southwest of 'Anderson's Prospect'. Sample 362697 (mg′ 0.69) is from the chilled base, and samples 362698, 362699 and 362700 (with mg′ values of 0.73, 0.75 and 0.72) were collected 1 m, 15 m and 50 m above the contact; sample 362700 has a relict cumulate texture, whereas the others are entirely metamorphic. Samples 362682, 362687 and 362689 (with mg′ values of 0.64, 0.65 and 0.69) have metamorphic textures and were collected from 10 m to 40 m below the upper contact of the component sill.

Sample 362661 (Analysis 11, Table 2; mg′ 0.60) is from the lowermost component sill exposed within the sill complex and has a metamorphic texture.

All seven of the mafic volcanic rocks analysed have metamorphic textures. Samples 362694, 362695 and 362663 (Analyses 15, 16 and 17, Table 2; mg′ values 0.52, 0.48 and 0.48) are respectively pillowed greenstone, massive greenstone and mafic tuff from unit C (Fig. 2), whereas 362684, 362685 and 362686 (Analyses 19, 20 and 21, Table 2; mg′ values 0.67, 0.67 and 0.61) are mafic tuff and hyaloclastite (362686, Analysis 21) within the main metasedimentary layer associated with 'Anderson's Prospect' in unit D (Fig. 2). The remaining sample (362652, Analysis 18, Table 2) also comes from unit D and is an altered mafic tuff (Figs 4c, 5c).

The analysed felsic volcanic rocks lack foliation and retain much of their primary texture. This is because many of the felsic layers, although having foliated marginal zones, possess relatively massive median zones. Samples 362656 and 362657 (Analyses 25 and 24, Table 2) are massive rhyolite and rhyodacitic tuff interlayered with the metasedimentary horizon at the boundary of units D and E (Fig. 2). Samples 362602, 362664 and 362709 (Analyses 23, 26 and 27, Table 2) are rhyolitic porphyries, the first two occurring at the base of the lowermost component sill in unit C (Fig. 2), and the last (362709, Analysis 27) lying along strike but being interlayered with pillowed greenstone. Of the remaining samples, 362601, 362732 and 362743

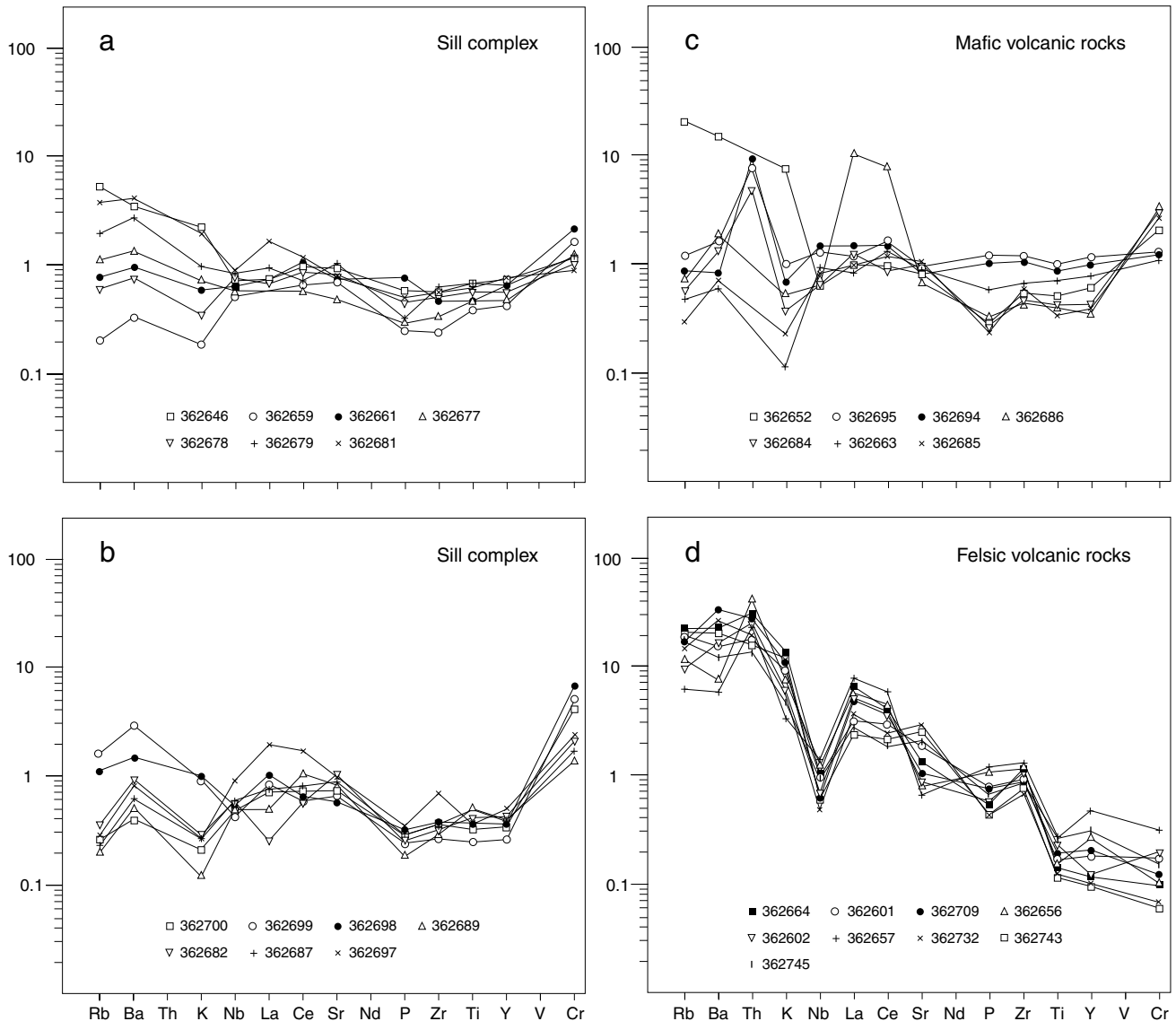

Fig. 5. MORB-normalised multi-element spider diagrams. **a** and **b**: Sill complex samples. **c**: Mafic volcanic samples. **d**: Felsic volcanic samples. Normalised after Pearce (1983).

(Analyses 22, 28 and 29, Table 2) are from rhyolitic porphyries in unit B (Fig. 2), and 362745 (Analysis 30, Table 2) is a rhyodacitic tuff from unit A (Fig. 2).

Alteration. The intensity of regional metamorphism precludes detailed evaluation of early alteration effects in any of the rock types, even though some degree of alteration should be anticipated. For example: (1) the peperitic contacts of the sill complex and the indications of soft-sediment deformation in the adjacent host rocks (above), are consistent with emplacement into water-charged rocks and associated hydrothermal circulation; (2) the high volatile contents of many of the analyses (Table 2) imply metasomatic alteration; and (3) pillow basalts and hyaloclastites commonly undergo alteration because of their mode of formation (e.g. Cas 1992). Despite this, the analyses in Table 2 for specific rock types are reasonably consistent and plot systematically on many of the petrological diagrams (below), irrespective of whether mobile or immobile and major or trace elements are employed. This consistency for samples from widely distributed sites suggests that neither pre-metamorphic alteration nor regional metamorphism has greatly distorted the chemical data, even though some redistribution of alkalies (Na, K, Rb and Ba) is probable (below).

Initial magma composition. A guide to the range of

initial compositions of magma pulses comprising the sill complex is provided by the chilled and finer-grained marginal phases within one or two metres from the contact. Samples 362697 (Analysis 6) and 362698 (7), and 362681 (2) and 362679 (3) (Table 2) are pairs of samples from two different contact zones. The high Na_2O contents of the contact samples, 362697 and 362681, imply a metasomatic contribution from the metasedimentary rocks across the contact, but this does not change the fact that the two pairs have widely differing mean mg′ values (approximately 0.71 and 0.56) and mean Ni contents (approximately 436 and 137 ppm). The data pairs respectively imply equilibrium with typical upper mantle mineralogies and some degree of fractional crystallisation of olivine, although interpretation can be complex (e.g. Wilson 1989); they are consistent with those from basaltic komatiites (Boryta & Condie 1990) and magnesian tholeiites (Cattell & Taylor 1990). In essence, provided that the two pairs represent liquid compositions, the component sills making up the sill complex represent magmatic pulses of significantly different gross composition.

Analysis of chemical data. On a Harker variation diagram of wt% $Na_2O + K_2O$ versus wt% SiO_2 (e.g. Wilson 1989, fig. 1.2), the mafic rocks (both from the sill complex and the lavas and tuffs) plot as sub-alkalic gabbros and basalts, and the felsic volcanic rocks as sub-alkalic rhyolites and dacites. The identifications are largely confirmed using the wt% SiO_2 versus log (Zr/TiO_2) plot of Winchester & Floyd (1977, fig. 2), although a few of the basaltic and sill complex samples lie in the alkali-basalt field. On diagrams of wt% K_2O and wt% Na_2O versus wt% silica (Middlemost 1975), these few samples are transitional in that they are alkalic with respect to Na_2O and sub-alkalic for K_2O. For all such cases, the samples are either from the contact zone of the sill, or from mafic hyaloclastite, and have most probably undergone Na enrichment (e.g. samples 362697 and 362698, Table 2). In essence, the only rocks that are not sub-alkalic are those affected by alteration.

The sill complex and mafic volcanic samples mainly plot as low-potassium tholeiites (fields A and B) on the Ti-Zr diagram of Pearce & Cann (1973, fig. 2). This most probably reflects the primary composition of the samples because their K_2O data are consistently low (Table 2). The dominantly tholeiitic character of the sill complex and mafic-volcanic samples is also clear on the Na_2O+K_2O – FeO* – MgO diagram (Fig. 3a), which conversely demonstrates the calc-alkaline affinity of the felsic rocks. These affinities are further shown on the Jensen diagram (Fig. 3b; Jensen 1976), where the majority of the sill complex and basaltic rocks plot as high-magnesium tholeiites (although three fall in the basaltic komatiite field), and the felsic rocks are calc-alkaline rhyolites and dacites (Fig. 3b).

Chondrite- and MORB-normalised multi-element spider diagrams (Thompson *et al.* 1984) for the various rock types are shown in Figs 4 and 5. The most obvious feature of both sets of spider diagrams is the similarity of the basaltic volcanic rocks to those of the sill complex. This is consistent with the proposed subvolcanic relationship between the basaltic and sill complex rocks. A second feature of both sets of spider diagrams (Figs 4, 5) is the distinctly different pattern of the felsic rocks. The difference in pattern is consistent with the felsic and mafic rocks respectively being calc-alkaline and tholeiitic. Such arc-style volcanism has been interpreted in terms of a type of compositionally zoned magma chamber that was kept in a liquid state by repeated inputs of mantle-derived mafic liquid (Smith 1979). Mafic volcanism could tap the lower part of the magma chamber and represent an over-supply of mantle-derived magma, whereas felsic volcanism could reflect the release, from the upper part of the chamber, of magma resulting from fractionation processes and assimilation of surrounding sialic material (Thurston 1990). Of course, if the calc-alkaline chemistry is solely ascribed to high-level assimilation, it then ceases to be a valid guide to an arc tectonic setting.

The chondrite-normalised spider diagrams for the mafic rocks (Fig. 4a–c) comprise patterns that are either flat or show a shallow downward tilt to the left with respect to LILE. The tilt is somewhat MORB-like and suggests a source that was relatively depleted in Rb, Ba and K (despite some possibility of alteration-related redistribution), whereas the flatter patterns imply that the majority of the elements analysed have retained near-chondritic proportions. Primitive MORB-like patterns and near-chondritic proportions of Ti, Zr, Y and Nb are characteristic of Archaean tholeiitic rocks, although few chemical discriminants for distinguishing between typical tholeiites and basaltic komatiites are universally applicable (Cattell & Taylor 1990; Hall & Hughes 1993). In the rocks from the sill complex (Fig. 4a, b) and even in the mafic volcanic samples (Fig. 4c), there is little or no indication of an enrichment in LILE and LREE relative to Nb (the subduction zone component – SZC – of Condie 1990), although samples 362652 (18) and 362686 (21) are notable exceptions. In contrast, the spider diagram for the felsic

volcanic rocks (Fig. 4d) possesses a distinct Nb trough (Nb depletion relative to the LILE and the LREE) and shows relative depletion of Ti against Zr and Y in a majority of samples.

With the exception of sample 362697 (6) (Fig. 5b) and samples 362652 (18) and 362686 (21) (Fig. 5c), the MORB-normalised spider diagrams for the sill complex and basaltic rocks (Fig. 5a–c) show the flat MORB-like to primitive MORB patterns of Archaean tholeiite (e.g. Snyder *et al.* 1990, fig. 9.7b; Type 1), or patterns similar to crustally contaminated komatiites (e.g. Hall & Hughes 1990, fig. 5.11). The three spider diagrams (Fig. 5a–c) show little indication of subduction-related processes in that they lack Nb and Ti negative anomalies (Wilson 1989; Condie 1990; Furnes *et al.* 1992). Similarly, with the possible exception of sample 362652 (18) (which is either crustally contaminated or altered), they lack evidence for crustal contamination, because the levels of enrichment of LILE and LREE are negligible. However, this interpretation of the LILE and LREE data could be misleading, because crustally contaminated komatiites and basaltic komatiites commonly have fractionated REE patterns, yet tend to show little enrichment in Rb and K, and generally lack a negative Nb anomaly (e.g. Hall & Hughes 1990). Although the matter remains inconclusive, limited support for this alternative possibility is provided by the patterns (Fig. 5a–c) differing from the average spider diagram for late Archaean greenstone belt metavolcanic assemblages, from which data for komatiites and basaltic komatiites have been excluded (Condie 1990).

Compared with the chondrite-normalised spider diagram (Fig. 4d) for the felsic volcanic rocks, the MORB-normalised plot (Fig. 5d) similarly shows Nb depletion relative to the LILE and the LREE (La and Ce), and, in some samples, Ti depletion against Zr and Y. These aspects, combined with the enrichment character of the more incompatible elements, are consistent with the felsic volcanic rocks having a calc-alkaline character (e.g. Furnes *et al.* 1992).

Most samples from the sill complex and the basaltic rocks plot in the basic field on the TiO_2 versus Zr diagram of Pharaoh & Pearce (1984), and thereby suggest that basalt-based tectonomagmatic discrimination diagrams may be applied to the analytical data. The use of such diagrams, even in the Phanerozoic, involves much uncertainty (e.g. Cas & Wright 1987; Pearce 1987; Wang & Glover 1992); and in the Archaean they could well be invalid (e.g. Wilson 1989; Cattell & Taylor 1990; Hall & Hughes 1993). Nevertheless, it is not uncommon for Archaean basalts to be classified in terms of modern basaltic types and their tectonic settings (e.g. Condie 1990; Boryta & Condie 1990). Thus, with due reservation, this practice will be followed.

The sill complex and basaltic rocks plot as island-arc tholeiites, with some overlap into the field of calc-alkaline basalts, on the TiO_2–MnO–P_2O_5 diagram of Mullen (1983). Similarly, they occupy the fields of island-arc basalts on the diagrams of Zr/Y versus Zr (Pearce & Norry 1989) and Ti/Zr versus Zr/Y (Condie 1990). Using a diagram of Ti/Zr versus Al_2O_3/TiO_2, Cattel & Taylor (1990) attempted to discriminate between komatiitic suites and Phanerozoic basaltic sequences. On this diagram, the sill complex and basaltic rocks plot in the fields of MORB and volcanic-arc basalts. However, approximately one-third of the samples (of both intrusive and extrusive rocks) also occupy the field comprising komatiite, komatiitic basalt and Archaean tholeiite, all of which derived from magmas that were probably erupted through Archaean continental crust (e.g. Cattell & Taylor 1990).

Discussion

Emplacement process

A sill complex, as opposed to a single intrusion that differentiated *in situ*, was recognised (Marshall & Schønwandt 1990) on the basis that: (1) the thinness, continuity and largely concordant nature of metasedimentary layers between sills are consistent with the layers being classical septa (e.g. Raudsepp & Ayre 1982); (2) interfingering with the host rocks characterises the outer limits of the complex, whereas a large forcefully emplaced intrusive body typically has marginal faulting and brecciation (e.g. Habekost & Wilson 1989); (3) large mafic intrusions typically have substantial contact-metamorphic aureoles and commonly contain contact-metamorphosed metasedimentary 'rafts', whereas here both are lacking (e.g. Habekost & Wilson 1989; Sipilä 1992); (4) the sill complex does not display the systematic distribution of the principal rock types that typifies *in situ* differentiation of a major intrusive body (e.g. Hatton & Von Gruenewalt 1990); (5) compositionally similar but very much thinner sills exist in other parts of the sequence away from the contact; (6) one example was found of an earlier sill being cut by a later one, even though this is uncommon for subvolcanic sill complexes (e.g. Raudsepp & Ayres 1982) and (7), the behaviour of the complex during regional fold-

ing is more in keeping with a well-layered sequence with marked mechanical anisotropy rather than with an integrated coherent intrusive.

In addition to the largely field-based guides (above), support is also provided by the geochemical data from contact zones in different parts of the sill complex (Table 2, samples 362679 and 362697). Although clearly part of the same magmatic system (Figs 4a, b, 5a, b) the contact samples themselves have distinctive major element chemistries and, in that they are interpreted as chilled facies, most probably constitute separate magmatic pulses. We shall therefore examine emplacement processes in the context of a progressively intruded sill complex rather than a single massive intrusion.

The sill complex was progressively emplaced within the dominantly metasedimentary sequence overlying a sequence of basaltic tuffs and lavas (Fig. 2). Although some of the septa are quite thick (up to 150 m), the majority are less than 20 m. This, together with the formation of peperitic rocks and chilled contacts, is in keeping with emplacement of the component sills into wet, probably poorly lithified, sedimentary material at shallow depths below the depositional interface (cf. Carlisle 1972; Raudsepp & Ayres 1982). In such sequences, successive sills tend to be intruded at progressively higher stratigraphic levels. This is because the position of the next sill is largely controlled by the interface between the contact-metamorphosed zone of the preceding sill and the overlying less-lithified sedimentary strata (Einsele 1980; Raudsepp & Ayres 1982). Indeed, strengthening of the sequence by intrusive and contact-metamorphic rocks is a factor in whether later magma forms intrusions or is erupted as flows (Carlisle 1972).

The rise of magma and its emplacement as sills is a complex process reflecting factors such as the depth and density relationships of the magma and potential host rocks, the dimensions of the feeder channel, the relative magnitudes of the horizontal (s_x) and vertical (s_z) stress components, the magmatic pressure (P_m), and the tensile strength (T_0) of the host materials (Williams & McBirney 1979). Nevertheless, in relation to the Guaymas Basin, Einsele (1980) demonstrated that upwelling magma will generally form sills through dilation when $P_m \geq P_s + T_0$ (where P_s is the effective overburden pressure exerted by the sediment load), and the magma reaches soft-sediment strata. He suggested that an alternating sill-sediment sequence is controlled by the thickness of the contact-metamorphosed or contact-lithified zone, the interval and volume of magmatic pulses, and the sedimentation rate; sills will continue to form (other things being equal) as long as sediment accumulation at least matches the vertical build-up of the last sill and its upper contact zone. Without drawing any tectonic analogy between the Guaymas Basin and an Archaean greenstone belt, we believe that the physical principles relating to the development of sill-sediment sequences (Einsele 1980) are equally applicable elsewhere.

The boundary between the sill complex and supracrustal rocks has the appearance of a replacement relationship rather than that of a dilational mode of emplacement (Fig. 2; p. 88). Einsele (1980) examined the decrease in porosity of sediment resulting from the expulsion of water from contact zones above and below sills. He demonstrated that the total water loss, expressed in terms of the height of an equivalent column of sediment, was of similar magnitude to the thickness of the sill. He therefore concluded that a sill could effectively create space for itself when intruding wet sediment. Even though these relationships are likely to be modified by later deformation and metamorphism, we believe that the process recognised by Einsele (1980; also see Kokelaar 1982) could have a bearing on the apparent replacement boundary between the sill complex and its host rocks.

Petrogenetic and tectonic aspects

The dominantly tholeiitic nature of the sill complex and mafic volcanic rocks of Arveprinsen Ejland is typical of most Archaean greenstone belts (e.g. Condie 1990). However, in that these rocks are high-magnesium tholeiites and include some basaltic komatiites (based on Fig. 2b and on the spider diagrams – Figs 4, 5), they most probably reflect decompressive melting of mantle with a higher potential temperature (T_p) than that forming the source of typical Archaean tholeiites (e.g. Bickle 1990; Cattell & Taylor 1990). But irrespective of this, there is some agreement that komatiitic basalts, typical Archaean tholeiites and, indeed, the igneous components of most greenstone belts, all probably erupted through continental crust (e.g. Bickle 1990; Cattell & Taylor 1990; Hall & Hughes 1990). Whether this means that they formed in ensialic rifts, or in arc-related settings such as intra-arc and back-arc basins is most uncertain (e.g. Condie 1990; Hall & Hughes 1990).

Thurston (1990) has suggested that Archaean greenstones contain four distinct stratigraphic associations. Insufficient data exist on the greenstones of Arveprin-

sen Ejland to unequivocally assign them to one of these groups, but in terms of the general descriptions presented (Thurston & Chivers 1989; Thurston 1990) they would seem to best fit the arc-volcanic association. This is supported by the existence of the sill complex, and by the calc-alkaline nature and subduction zone component (SZC – Condie 1990) of the felsic volcanic rocks (Figs 3, 4, 5). It is further supported by various tectonomagmatic discrimination diagrams (above).

Megacrystic plagioclase ($An_{85\pm5}$) is a common feature of many Archaean tholeiitic flows, sills and dykes (Green 1975; Phinney *et al.* 1988); and such are present in parts of the Arveprinsen sill complex. Phinney *et al.* (1988, p. 1320) proposed a four-stage model to explain the formation of anorthositic complexes and the megacryst-bearing flow and intrusive bodies. The main points of their model involve: (1) high-pressure fractionation of olivine and pyroxene from a picritic or komatiitic mafic melt; (2) pulses of the fractionated, less-dense melt rapidly ascending to a low-pressure (1–2 kb) chamber, in which corresponding pulses of plagioclase crystallisation reflect depressurisation and undercooling; (3) the megacrysts forming cumulate layers within a melt which is fractionating along a tholeiitic trend and ultimately crystallises as an anorthosite complex; and (4) the pulsed input inducing periodic expulsion of megacryst-bearing melt to form flows, sills and dykes.

If this model (Phinney *et al.* 1988) is applied at Arveprinsen Ejland, then the megacryst bearing sills within the sill complex would equate with expulsions of melt from the low-pressure chamber. It therefore follows that, provided the other components of the sill complex were expelled from the same magma chamber (and this would seem to be supported by the chemical data), an indication exists of the dynamic complexity, in terms of degree of fractionation and residence times, that characterised both the high- and low-pressure magma chambers. Thus, as described above and similarly reported by Phinney *et al.* (1988), the component sill might, in places, contain megacryst-rich cumulate layers, whereas in others, sparse, relatively small megacrysts (1 to 3 cm), appear to have grown *in situ* in equilibrium with the melt.

A final point stemming from the model (Phinney *et al.* 1988) is that the sill complex was most probably emplaced at pressures well below 1 kb. This is consistent with Einsele (1980), who suggested that, in the Gulf of California, the upper limit of basaltic sill emplacement is in the order of 2 to 3 km below sea level and 150 to 200 m below the sea-sediment interface. It is also consistent with Kokelaar (1982, 1986), who suggested that the fluidisation of wet sediment at peperitic contacts was improbable at depths below about 3 km of seawater or 1.6 km of wet sediment. Although speculative, these data imply that the sill complex could have been progressively emplaced beneath 2 to 2.5 km of seawater and considerably less than 0.5 km of wet sediment.

Conclusions

The Archaean sill complex of north-eastern Arveprinsen Ejland constitutes a multiple, essentially concordant intrusion within a dominantly metasedimentary sequence overlying massive and pillowed lavas, and mafic tuffs. Field observations and chemical data are consistent with the component sills of the sill complex being emplaced as an upward-younging sequence into wet, poorly lithified sedimentary strata, at shallow levels below the water-sediment interface. Magma intruded to form the component sills when, for each sill, the magmatic pressure equalled or exceeded the *effective* overburden pressure plus the vertical tensile strength of the host materials at the level of intrusion (i.e. $P_m \geq P_s + T_0$). This condition was most probably induced by the sudden decrease in T_0 at the interface between contact-lithified rock and overlying poorly lithified strata. Determinants of the thickness of the sedimentary septa between component sills principally comprised the thickness of the contact-lithified zone above the previously emplaced sill, the rate of sedimentation, and the hiatus until the next magmatic pulse. The discordant, replacement-like boundary between the sill complex and supracrustals is believed to partly reflect the capacity of a sill to create space for itself (other than by dilation) when intruding wet sediment.

The sill complex and petrogenetically related mafic volcanic rocks are high-magnesium tholeiites and basaltic komatiites (on a Jensen plot; Jensen 1976) with a continental crust influence. Together with the calc-alkaline felsic volcanics, they probably comprise an ensialic arc-volcanic association. The sill complex was emplaced from a low-pressure magma chamber, in turn linked to a high-pressure chamber. Both chambers were dynamically complex in terms of the degree of fractionation and residence times of the many small pulses of magma that passed through them. Progressive emplacement of the sill complex probably happened beneath 2 to 2.5 km of seawater and substantially less than 0.5 km of wet sediment.

Acknowledgements

John Korstgård paved the way for BM to work with the Geological Survey of Greenland on Arveprinsen Ejland, as part of the Disko Bugt Project. BM appreciates the support of The University of Technology, Sydney for allowing him to spend time in Greenland and providing financial assistance. He also acknowledges the logistic and financial support of the Geology Department at Aarhus University, Denmark, where he stayed on returning from Greenland. Finally, he expresses appreciation to Heikki Papunen at Turku University, Finland, for providing space whilst this paper was being assembled, and to Franco Mancini for helping to process the chemical data and providing stimulating discussion.

References

Bickle, M.J. 1990: Mantle evolution. In: Hall, R.P. & Hughes, D.J. (eds): Early Precambrian basic magmatism, 111–135. London: Blackie.

Boryta, M. & Condie, K.C. 1990: Geochemistry and origin of the Archaean Beit Bridge complex, Limpopo Belt, South Africa. Journal of the Geological Society (London) **147**, 229–239.

Brooks, E.R., Wood, M.W. & Garbutt, P.L. 1982: Origin and metamorphism of peperite and associated rocks in the Devonian Elwell Formation, northern Sierra Nevada, California. Bulletin of the Geological Society of America **93**, 1208–1231.

Busby-Spera, C. & White, J.D.L. 1987: Variation in peperite textures associated with differing host-sediment properties. Bulletin of Volcanology **49**, 765–775.

Carlisle, D. 1972: Late Paleozoic to Mid-Triassic sedimentary-volcanic sequence on northeastern Vancouver Island. Geological Survey of Canada Paper **72-1 B**, 24–30.

Cas, R.A.F. 1992: Submarine volcanism: eruption styles, products, and relevance to understanding the host-rock successions to volcanic-hosted massive sulphide deposits. Economic Geology **87**, 511–541.

Cas, R.A.F. & Wright, J.V. 1987: Volcanic successions – modern and ancient. A geological approach to processes, products and successions. 529 pp. London: Allen & Unwin.

Cattell, A.C. & Taylor, R.N. 1990: Archaean basic magmas. In: Hall, R.P. & Hughes, D.J. (eds): Early Precambrian basic magmatism, 11–39. London: Blackie.

Condie, K.C. 1990: Geochemical characteristics of Precambrian basaltic greenstones. In: Hall, R.P. & Hughes, D.J. (eds): Early Precambrian basic magmatism, 40–55. London: Blackie.

Einsele, G. 1980: Mechanism of sill intrusion into soft sediment and expulsion of pore water. In: Curray J.R. & Moore D.G. (eds): Initial reports DSDP, **64**, 1169–1176. Washington: U.S. Government Printing Office.

Escher, A. & Burri, M. 1967: Stratigraphy and structural development of the Precambrian rocks in the area north-east of Disko Bugt, West Greenland. Rapport Grønlands Geologiske Undersøgelse **13**, 28 pp.

Furnes, H., Pedersen, R.B., Hertogen, J. & Albrektsen, B.A. 1992: Magma development of the Leka Ophiolite Complex, central Norwegian Caledonides. Lithos **27**, 259–277.

Garde, A.A. 1994: Precambrian geology between Qarajaq Isfjord and Jakobshavn Isfjord, West Greenland, 1:250 000. Copenhagen: Geological Survey of Greenland.

Green, N.L. 1975: Archaean glomeroporphyritic basalts. Canadian Journal of Earth Sciences **12**, 1770–1784.

Habekost, E.M. & Wilson, R. 1989: Raft-like metabasaltic inclusions in the Fongen–Hyllingen layered intrusive complex, Norway, and their implications for magma chamber evolution. Journal of Petrology **30**, 1415–1441.

Hall, R.P. & Hughes, D.J. 1990: Noritic magmatism. In: Hall, R.P. & Hughes, D.J. (eds): Early Precambrian basic magmatism, 833–910. London: Blackie.

Hall, R.P. & Hughes, D.J. 1993: Early Precambrian crustal development: changing styles of mafic magmatism. Journal of the Geological Society (London) **150**, 625–635.

Härme, M. 1980: Kivilajikartan selitys, with English summary. Suomen geologinen yleiskartta – The general geological map of Finland, Lehti-Sheet C1-D1. 95 pp. Helsinki: Geological Survey of Finland.

Hatton, C.J. & Von Gruenewalt, G. 1990: Early Precambrian layered intrusions. In: Hall, R.P. & Hughes, D.J. (eds): Early Precambrian basic magmatism, 56–82. London: Blackie.

Irvine, T.N. & Baragar, W.R.A. 1971: A guide to the chemical classification of the common volcanic rocks. Canadian Journal of Earth Sciences **8**, 523–548.

Jaques, A.L. 1976: An Archaean tholeiitic layered sill from Mt Kilkenny, Western Australia. Journal of the Geological Society of Australia **23**, 157–168.

Jensen, L.S. 1976: A new cation plot for classifying subalkalic volcanic rocks. Ontario Geological Survey Miscellaneous Paper **66**, 22 pp.

Kalsbeek, F., Taylor, P.N. & Pidgeon, R.T. 1988: Unreworked Archaean basement and Proterozoic supracrustal rocks from northeastern Disko Bugt, West Greenland: implications for the nature of Proterozoic mobile belts in Greenland. Canadian Journal of Earth Sciences **25**, 773–782.

Knudsen, C., Appel, P.W.U., Hageskov, B. & Skjernaa, L. 1988: Geological reconnaissance in the Precambrian basement of the Atâ area, central West Greenland. Rapport Grønlands Geologiske Undersøgelse **140**, 9–17.

Kokelaar, B.P. 1982: Fluidization of wet sediments during the emplacement and cooling of various igneous bodies. Journal of the Geological Society (London) **139**, 21–33.

Kokelaar, B.P. 1986: Magma-water interactions in subaqueous and emergent basaltic volcanism. Bulletin of Volcanology **48**, 275–289.

Marshall, B. & Schønwandt, H.K. 1990: Geological investigations of Archaean supracrustals, Arveprinsen's Ejland, Disko Bugt, central west Greenland, 41 pp. Unpublished report, Geological Survey of Greenland, Copenhagen.

Middlemost, E.A.K. 1975: The basalt clan. Earth-Science Reviews **11**, 337–364.

Mullen, E.D. 1983: A minor element discriminant for basaltic rocks of oceanic environments and its implications for petrogenesis. Earth and Planetary Science Letters **62**, 53–62.

Naldrett, A.J. & Mason, G.D. 1968: Contrasting Archaean ultramafic bodies in Dundonald and Clergue Townships, Ontario. Canadian Journal of Earth Sciences **5**, 111–143.

Pearce, J.A. 1983: Role of the sub-continental lithosphere in magma genesis at active continental margins. In: Hawkesworth C.L. & Norry M.J. (eds): Continental basalts and mantle xenoliths, 230–249. Nantwich, UK: Shiva Publishing Ltd.

Pearce, J.A. 1987: An expert system for the tectonic characterization of ancient volcanic rocks. Journal of Volcanolgy and Geothermal Research **32**, 51–65.

Pearce, J.A. & Cann, J.R. 1973: Tectonic setting of basic volcanic rocks determined using trace element analyses. Earth and Planetary Science Letters **19**, 290–300.

Pearce, J.A. & Norry, M.J. 1979: Petrogenetic implications of Ti, Zr, Y, and Nb variations in volcanic rocks. Contributions to Mineralogy and Petrology **69**, 33–47.

Pharaoh T.C. & Pearce, J.A. 1984: Geochemical evidence for the geotectonic setting of Early Proterozoic metavolcanic sequences in Lapland. Precambrian Research **10**, 283–309.

Phinney, W.C., Morrison, D. & Maczga, D.E. 1988: Anorthosites and related megacrystic units in the evolution of Archaean crust. Journal of Petrology **29**, 1283–1323.

Raudsepp, M. & Ayres, L.D. 1982: Emplacement and differentiation of an Archaean subvolcanic metapyroxenite-metagabbro sill in the Favourable Lake area, northwestern Ontario. Canadian Journal of Earth Sciences **19**, 837–858.

Sipilä, P. 1992: The Caledonian Halti–Ridnitsohkka igneous complex in Lapland. Bulletin of the Geological Survey of Finland **362**, 5–75.

Smith, R.L. 1979: Ash-flow magmatism. Geological Society of America Special Paper **180**, 5–27.

Snyder, G.L., Hall, R.P., Hughes, D.J. & Ludwig, K.R. 1990: Early Precambrian basic rocks of the USA. In: Hall, R.P. & Hughes, D.J. (eds): Early Precambrian basic magmatism, 191–220. London: Blackie.

Suominen, V. 1988: Radiometric ages on zircons from a cogenetic gabbro and plagioclase porphyrite suite in Hyvinkää, southern Finland. Bulletin of the Geological Society of Finland **60**, 135–140.

Thompson, R.N., Morrison, M.A., Hendry, G.L. & Parry, S.J. 1984: An assessment of the relative roles of crust and mantle in magma genesis. Philosophical Transactions of the Royal Society of London **A310**, 549–590.

Thurston, P.C. 1990: Early Precambrian basic rocks of the Canadian Shield. In: Hall, R.P. & Hughes, D.J. (eds): Early Precambrian basic magmatism, 221–247. London: Blackie.

Thurston, P.C. & Chivers, K.M. 1990: Secular variation in greenstone sequence development emphasizing Superior Province, Canada. In: Gaal, G. & Groves, D.I. (eds): Precambrian ore deposits related to tectonics. Precambrian Research **46**, 21–58.

Wang, P. & Glover III, L. 1992: A tectonics test of the most commonly used geochemical discriminant diagrams and patterns. Earth-Science Reviews **33**, 111–131.

Williams, H. & McBirney, A.R. 1979: Volcanology, 397 pp. San Francisco: Freeman, Cooper & Co.

Wilson, M. 1989: Igneous petrogenesis, 466 pp. London: Unwin Hyman.

Winchester, J.A. & Floyd, P.A. 1977: Geochemical discrimination of different magma series and their differentiation products using immobile elements. Chemical Geology **20**, 325–343.